PROJECT

New Catalysts for Direct Methanol Oxidation Fuel Cells

Principal Investigator: Radoslav Adzic   Signature:

Staff: N. Marinkovic

Partner: International Fuel Cells Corporation, Inc.

Final Report

Project Duration: May 1995-May 1998

UNLIMITED RELEASE

DISCLAIMER

DISCLAIMER

Portions of this document may be illegible in electronic image products. Images are produced from the best available original document.

Abstract

A new class of efficient electrocatalytic materials based on platinum – metal oxide systems has been synthetized and characterized by several techniques. Best activity was found with $NiWO_4$-, $CoWO_4$-, and RuO_2- supported platinum catalysts. A very similar activity at room temperature was observed with the electrodes prepared with the catalyst obtained from International Fuel Cells Inc. for the same Pt loading. Surprisingly, the two tungstates *per se* show a small activity for methanol oxidation without any Pt loading. Synthesis of $NiWO_4$ and $CoWO_4$ were carried out by solid-state reactions. FTIR spectroscopy shows that the tungstates contain a certain amount of physically adsorbed water even after heating samples at 200 °C. A direct relationship between the activity for methanol oxidation and the amount of adsorbed water on those oxides has been found. The Ru(0001) single crystal shows a very small activity for CO adsorption and oxidation, in contrast to the behavior of polycrystalline Ru.

In situ extended x-ray absorption fine structure spectroscopy (EXAFS) and x-ray absorption near edge spectroscopy (XANES) showed that the OH adsorption on Ru in the Pt-Ru alloy appears to be the limiting step in methanol oxidation. This does not occur for $Pt-RuO_2$ electrocatalyst, which explains its advantages over the Pt-Ru alloys. The IFCC electrocatalyst has the properties of the Pt-Ru alloy.

Project Objectives

There were two objectives of this project. The first was to synthesize and characterize a new class of efficient electrocatalytic materials based on platinum – metal oxide systems. The second one was to clarify the difference in the behavior of the Pt-Ru alloy and Pt-Ru oxide electrocatalysts, since the first one has been the best electrocatalyst system commercially available so far and there were indications that the other offered some improvement.

Methanol as a potential fuel in fuel cells brings about several advantages over hydrogen, including storage capacity, specific cost and safety of use. However, the key problem in developing of methanol fuel cells is the inadequate activity of the anode catalyst. Metallic platinum is sufficiently active for a partial oxidation of methanol. Its surface, however, becomes rapidly blocked with the strongly bound products of this partial oxidation, predominantly carbon monoxide (CO). Further oxidation of CO to CO_2 requires a reaction of CO with oxygen-containing species. These species are formed in oxidation of water on platinum, for which a substantial overpotential is required. Ruthenium is oxidized to RuOH on more negative potentials so that the oxidation of CO to CO_2 on Pt-Ru alloys occurs at lower potentials. However, the activity of Pt-Ru alloy systems is still unsatisfactory and their cost appears prohibitively high. Improvement of the activity of electrocatalysts and decreasing their load are needed before the commercialization of the direct methanol fuel cells becomes feasible.

The initial step in methanol oxidation on Pt is the adsorption of the organic molecule on the catalyst's surface. In our view, alloying platinum with ruthenium changes the electronic property of platinum, making it less active for the adsorption of methanol, the first critical step of the reaction. On the other hand, it was expected that supporting Pt on metal oxide surfaces should not cause a pronounced change of the electronic properties of platinum since the catalyst-support interactions are usually less strong than the interactions of the alloying components. Therefore, the change in the electronic properties of Pt is expected to be decreased which would prevent a loss of activity for methanol adsorption caused by alloying. The oxygen-containing species, necessary for CO oxidation, would be supplied from hydroxyl or water strongly interacting with the oxide surfaces. The "spillover" of CO to M-OH or $M-H_2O_{ads}$, or of OH to Pt sites, is expected to occur to make this reaction possible. The consumed oxygen-containing species could be easily replenished by reaction of the oxide surface with water.

Selection and Synthesis of Oxides

Several metal oxides were tested during this project. For selecting a potential candidate, the following factors were taken into account: first, the oxide has to be stable in strongly acidic solution. Further, the oxide needs to be able to provide the oxygen (in form of OH or H_2O_{ads}) and finally, it needs to readily readsorb H_2O or OH. After initial screening, several transition-metal oxides, mixed oxides and one chalchogenide were selected. Most oxides were purchased (Aldrich, CERAC) and used without further refining. Some of potentially good candidates, unavailable from external sources, were synthesized.

The best results were obtained with $NiWO_4$ and $CoWO_4$ compounds and both, commercial and synthesizes samples of these oxides were tested. Synthesis of $NiWO_4$ and $CoWO_4$ were carried out by solid-state reactions of corresponding metal nitrates and ammonium tungstate, at temperatures lower than that used in commercial synthesis. This procedure yields a smaller grain particle size of the oxides and improves the electrochemical activity of the oxide substrate for methanol oxidation, as shown below.

Characterization

<u>Physical methods:</u>

Synthesized oxides were characterized by x-ray diffraction to confirm their structure. It has been found that the synthesis of nickel and cobalt tungstates can proceed at 600 °C. X-ray diffraction spectrum shows that the obtained powder is over 99% $NiWO_4$ (or $CoWO_4$). The impurities, mostly NiO or CoO that have not been reacted, can be easily dissolved in H_2SO_4. After the cleaning x-ray diffraction reveals no trace impurities, producing a spectrum identical to that of commercial tungstates.

BET gas adsorption data were used to measure the average particle diameter of the oxides. It was shown that the electrochemical activity of these oxides depends inversely on the particle size. Synthesized oxide particles were shown to have several times smaller diameter than that of commercial samples. Combining the synthesis procedure with ball milling, oxide particles of 0.3μm in diameter were obtained.

Electrode preparation:

The electrodes were prepared by chemical or electrochemical deposition of Pt particles on the substrate. For oxide support, an appropriate amount of Pt in the form of H_2PtCl_6 was added, followed by the reduction of Pt by a reduction agents ($NaBH_4$, H_2 or citric acid). The best results were obtained by reduction with a dilute solution (0.01M) of $NaBH_4$ with strong agitation. Pt/RuO_2 electrodes were prepared by mixing appropriate concentrations of H_2PtCl_6 and $RuCl_3$ in 50% alcohol, followed by adding the solution dropwise into a cooled alkaline solution of $NaBH_4$ with strong agitation.

The powdered catalysts were mixed with an appropriate amount of carbon (Vulcan X75), previously mixed with Teflon (37% wt.) and pressed onto a nickel net with electrochemically deposited gold film, or onto a gold thin sheet. Before pressing, each gold-covered nickel net was electrochemically tested in a acidic methanol solution for stability of the gold thin layer. Since gold has no oxidation capability for the methanol oxidation, if a current other than charging of the double layer is detected, such a gold/nickel net was discarded.

Electrochemical measurements:

Electrochemical techniques were used to determine the activity of prepared electrocatalysts. Kinetics of methanol oxidation has been measured with the prepared electrodes and their activity compared with the activity of the samples obtained from IFCC. Electrochemical activities of these oxides were checked before deposition of Pt. Various loads of Pt on several oxides and Pt supported on mixed oxides were studied. Best activity was found with $NiWO_4$-, $CoWO_4$-, and RuO_2- supported platinum catalysts.

6

Surprisingly, the two tungstates *per se* show a small activity for methanol oxidation without any Pt loading. Figure 1 shows the electrochemical oxidation of methanol on $NiWO_4$. The oxidation starts at 0.6 V, i.e. at the potential close to the one found for a platinum electrode. Although the activity is low, this finding demonstrates that $NiWO_4$ can be an interesting support. This also indicates that further study of oxides as supports for Pt may be promising.

Figure 2 shows the oxidation of methanol on samples prepared by dispersing platinum particles on commercial $NiWO_4$ (particle size of 45 μm) and on synthesized $NiWO_4$. The latter was ball milled down to the particle size 0.3 μm. The sweep in anodic direction is only shown. It is seen that the onset of methanol oxidation strongly depends on the particle size of tungstate. The samples with smaller grains have the onset of methanol oxidation shifted by 120 mV to the less positive potentials. The current density of over 100 mA/cm^2 is reached at 0.6 V. Further refinement of the particle size of the tungstate is likely to shift the onset of oxidation to even lower potentials. With further optimization of the system, in particular of the electrode structure, an increase in the activity can be expected and the Pt-metal oxide samples can probably reach or surpass the activity of Pt-Ru alloys.

Further improvement of the methanol oxidation kinetics was achieved by mixing $NiWO_4$ with 0.3 μm RuO_2 and Pt. Figure 3 shows that the current density of the order of 150 mA/cm^2 can be obtained at 0.6 V with a sample consisting of 90%$NiWO_4$, 10% RuO_2 and Pt. A very similar activity at room temperature was observed with the electrodes prepared with the catalyst obtained from IFCC for the same Pt loading. At somewhat more positive potentials, the oxide-supported catalysts show even slightly better activities.

This finding prompted investigation of the Pt-RuO$_2$ electrodes by electrochemical and XANES techniques (vide infra).

Spectroscopic measurements:

FTIR: Fourier transform infrared spectroscopy was used to confirm that water strongly interacts with the NiWO$_4$ and CoWO$_4$ oxide surfaces. The attenuated total reflection configuration was used for studying high area oxide surfaces. It was shown that the tungstates contain a certain amount of physically adsorbed water even after heating samples at 200 °C. For several samples investigated there was a direct relationship between the activity for methanol oxidation and the amount of adsorbed water on those oxides. This information is relevant for the function of the oxides as a support for Pt in methanol oxidation and confirms the validity of our approach to the problem.

In situ infrared spectroscopy was also used to study methanol and CO oxidation on platinum covered by a submonolayer of ruthenium and on ruthenium electrodes. The spectra obtained on polycrystalline Ru and Pt confirm electrochemical data regarding the onset potential of the CO oxidation. In methanol oxidation on submonolayer coverages of Ru on Pt, in addition to adsorbed CO, adsorbed carboxylic species have been observed. Some experiments were also conducted with a well-ordered single crystal Ru(0001) surface and compared with the data for polycrystalline Ru and with Pt(111) which has the same hexagonal arrangement of atoms at the surface the Ru(0001) surface. While both polycrystalline Pt and Pt(111), as well as polycrystalline ruthenium, show an appreciable activity toward CO oxidation, the surface of the Ru(0001) single crystal shows a very

small activity. This was found by electrochemical techniques and confirmed by IR data. SNIFTIR spectra for the CO oxidation on Ru(poly) and Ru(0001) are presented in Figs. 4a and 4b. CO is strongly bound on Ru(poly) until the potential of about 0.3 V, indicated by the strong, bipolar-shaped band with a maximum at ~2000 cm^{-1}, Fig. 4a. At more positive potentials CO is oxidized and the CO coverage decreases. At the same time a strong, narrow band at ~2340 cm^{-1}, due to the solvated CO_2 is observed. On the other hand, the coverage of CO is hardly observable on Ru(0001) at all potentials, and consequently no CO_2 could be detected in the spectrum, Fig. 4b. This finding warrants further study of the role of the Ru orientation for CO adsorption and in determining the activity of the Pt-Ru systems.

X-ray adsorption studies: In situ extended x-ray absorption fine structure spectroscopy (EXAFS) and x-ray absorption near edge spectroscopy (XANES) showed that there is an important difference in the behaviors of the Pt-Ru alloys and Pt-RuO$_2$ electrocatalysts. *In situ* XANES spectroscopy by measuring the platinum L$_3$ edge showed a strong interaction between the two metals in the alloy, while the Pt-RuO$_2$ sample had a much lower perturbation of Pt. This observation confirms our previous interpretation of electrochemical data involving the changes of the methanol adsorption on Pt upon alloying. In addition, by measuring the ruthenium edge during the course of methanol oxidation, the changes in ruthenium oxidation state was observed and the behavior of the two systems compared. Important difference in the behavior of Pt-Ru alloys and Pt-RuO$_2$ system during methanol oxidation have been demonstrated. Figure 5 shows the comparison of the ruthenium edge XANES spectra on the Pt-Ru alloy and Pt-RuO$_2$

samples at different electrode potentials. At the most negative potentials (0.0 V), both samples show that ruthenium is oxidized. At 0.54 V, where methanol oxidation current densities are substantial for both samples, the Pt-Ru alloy sample shows that ruthenium oxidation state is close to the metallic Ru. On the other hand, the $Pt-RuO_2$ catalyst shows no such limitation, as the surface oxygen-containing species are readily available on the RuO_2 surface and no decrease in the Ru-OH signature in spectra was observed. Therefore, the OH adsorption on Ru in the Pt-Ru alloy appears to be the limiting step in methanol oxidation. As it can be seen from Fig. 5, the three curves for methanol oxidation on the Pt/RuO_2 sample at three different potentials lie below the Ru black standard, confirming that the Ru oxidation state is practically unchanged during the methanol oxidation. This difference in the behavior of the two catalysts explains the advantages of the $Pt-RuO_2$ electrodes over Pt-Ru alloys, observed in the electrochemical measurements at higher positive potentials (see Fig. 3). These results show that the RuO_2 supported Pt is a better electrocatalyst for methanol oxidation than the Pt-Ru alloys.

The IFCC electrocatalyst has been characterized by both, XANES and EXAFS techniques. The results that the IFCC electrocatalyst has properties of the Pt-Ru alloy.

Significant Accomplishments

A synthesis of a new class of catalysts for direct methanol fuel cells based on the Pt-metal oxides systems has been realized. The activity of the $Pt-NiWO_4$ and $Pt-CoWO_4$ electrocatalysts is not only comparable but is higher at larger overpotentials than that of commercial samples. These electrocatalysts have not been optimized. There is a possibility for further improvement, in particular regarding grain size of the support and the electrode

structure. This indicates the Pt-metal oxide systems should be further explored. The system with mixed oxides, containing 5-10% of Ru_2O, shows even better characteristics. The amount of ruthenium is substantially reduced, if not completely eliminated, with respect to the best Pt-Ru alloy catalysts containing 50% Ru.

The results of the project demonstrated that the $Pt-RuO_2$ electrocatalysts have advantages over the Pt-Ru alloy electrocatalysts and explained the difference in the behavior on the basis of the XANES and EXAFS data.

FTIR spectroscopy measurements demonstrated that adsorbed H_2O layers are present on surfaces of some oxides even after heating at 200 °C. Activity of oxide-supported Pt electrocatalysts for methanol oxidation is related to the amount of adsorbed water. *In situ* FTIR spectroscopy measurements revealed that there is a relationship between the Ru surface orientation and the amount of adsorbed CO. Both information indicate that these are directions for future studies of electrocatalysts for methanol oxidation.

Significant Problems

The major problem in the project was to synthesize the micro particles of Ni- or Co-tungstates. The results indicate that the catalytic activity can be considerably increased with further decrease of the particle size of these oxides. That, however, could not be obtained by simple ball-milling procedure used and requires a considerable synthetic effort.

Industry Benefits

Several benefits for the industry resulted from this project. The information on the distinct advantage of the Pt-RuO_2 electrocatalyst over the Pt-Ru alloy suggests that the IFCC could improve their fuel cells by switching over to the Pt-RuO_2 system. A characterization of the IFCC electrocatalyst by EXAFS and XANES techniques provides useful information for comparison with other systems and evaluation of the electrocatalysts performance. The results on the new Pt-metal oxide electrocatalysts obtained in this project may be a starting point for further work on these promising systems.

Laboratory Benefits

A new direction in fuel cell electrocatalysis has been established and promising results were obtained. The hardware for the work with high surface area electrodes has been developed. In situ FTIR spectroscopy has been implemented and diffuse reflectance technique for a high surface area systems became available. One patent is currently under evaluation. Further understanding of the principles of methanol oxidation has been achieved. The results from this research could help future fuel cells, batteries and carbon dioxide reduction projects in the Laboratory.

Recommended Follow-on Work and its Potential Benefits

Further work should focus on finding a method to reduce the particle size of Ni- and Co-tungstates. A success could lead to further optimization of the electrocatalyst, leading to its higher activity. Mixed oxides and several other promising oxide materials
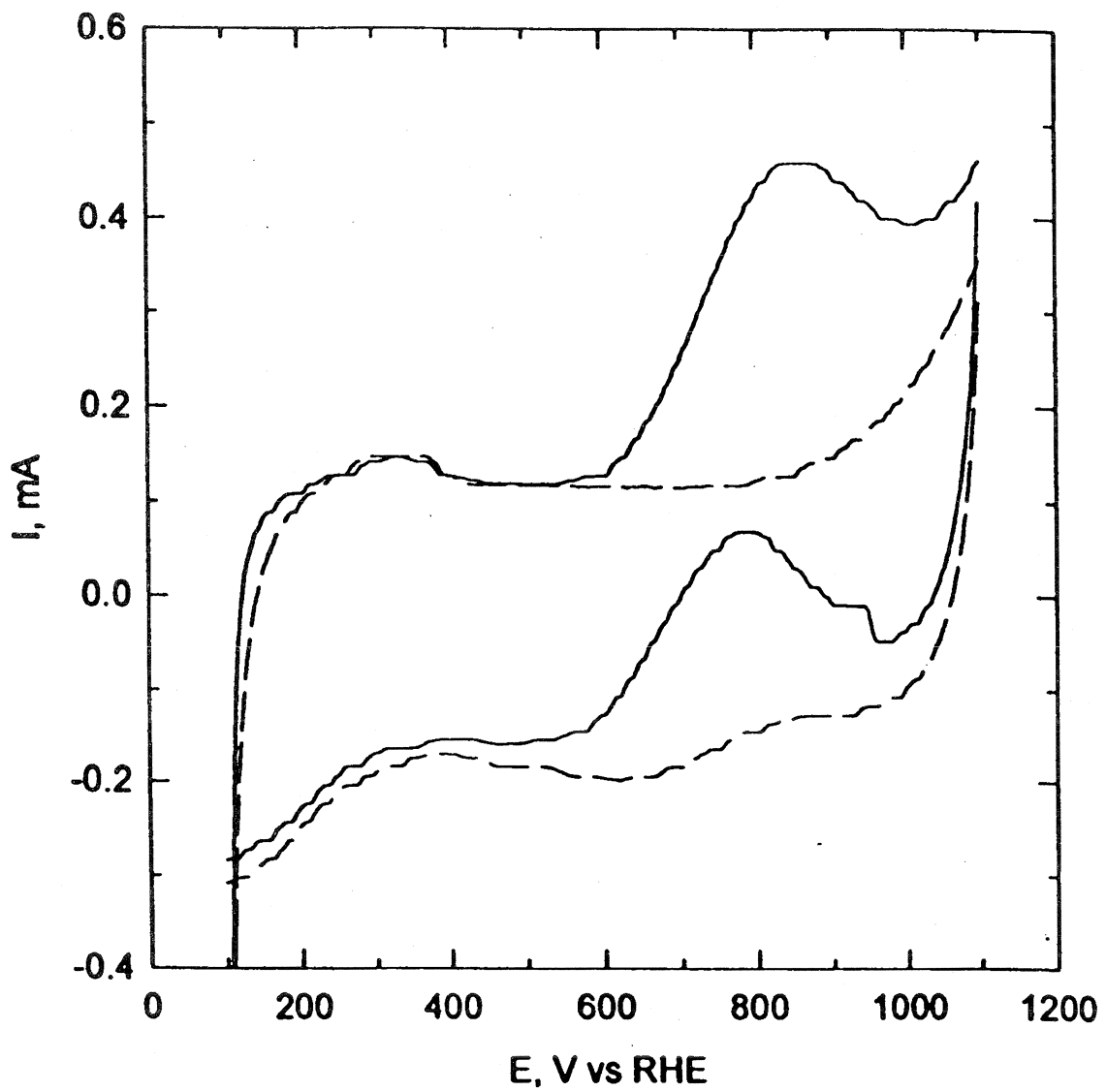
should be investigated as a support for Pt. This work would provide a more complete assessment of the possibilities and intrinsic activities of Pt-metal oxide electrocatalysts.
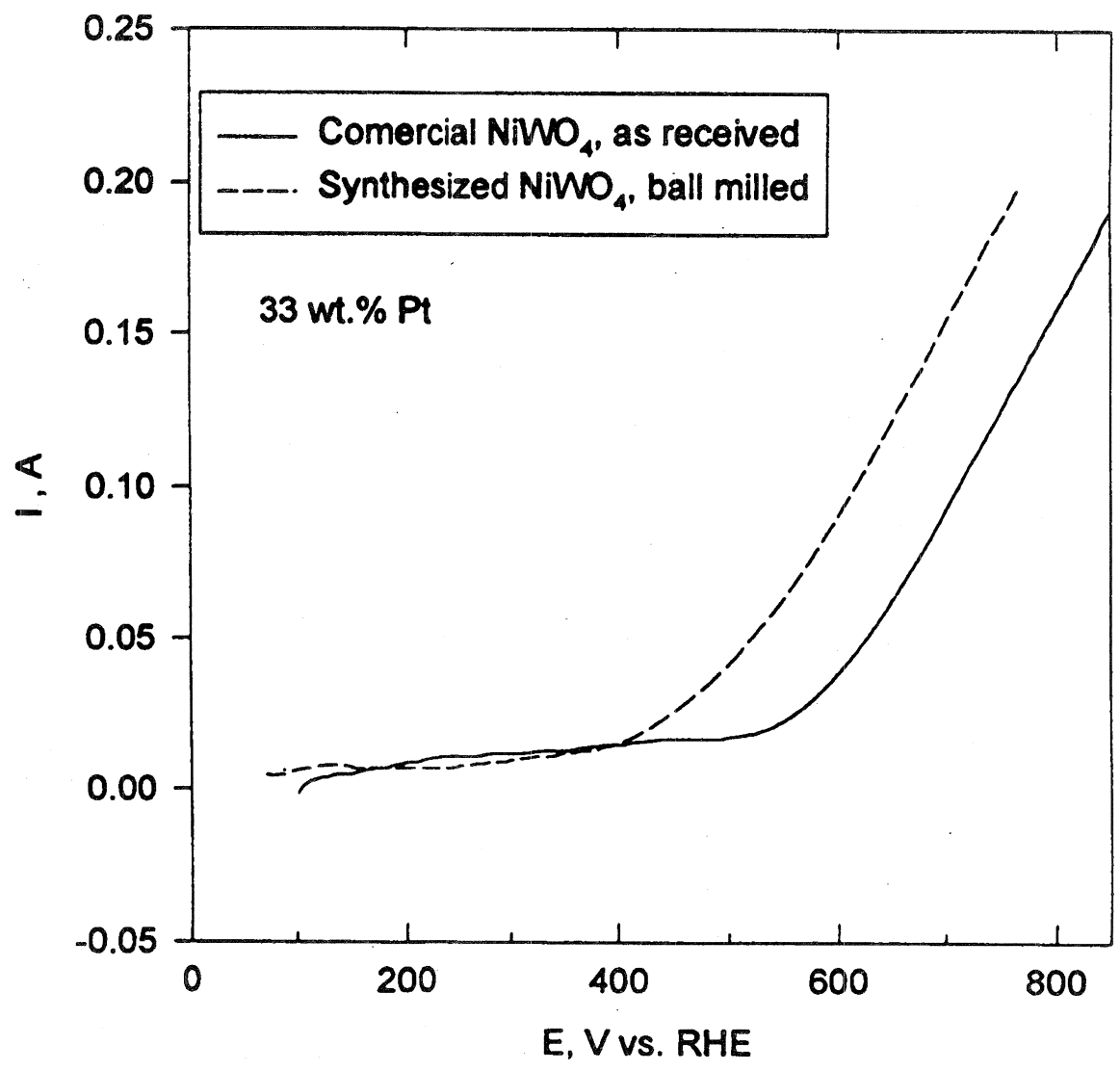
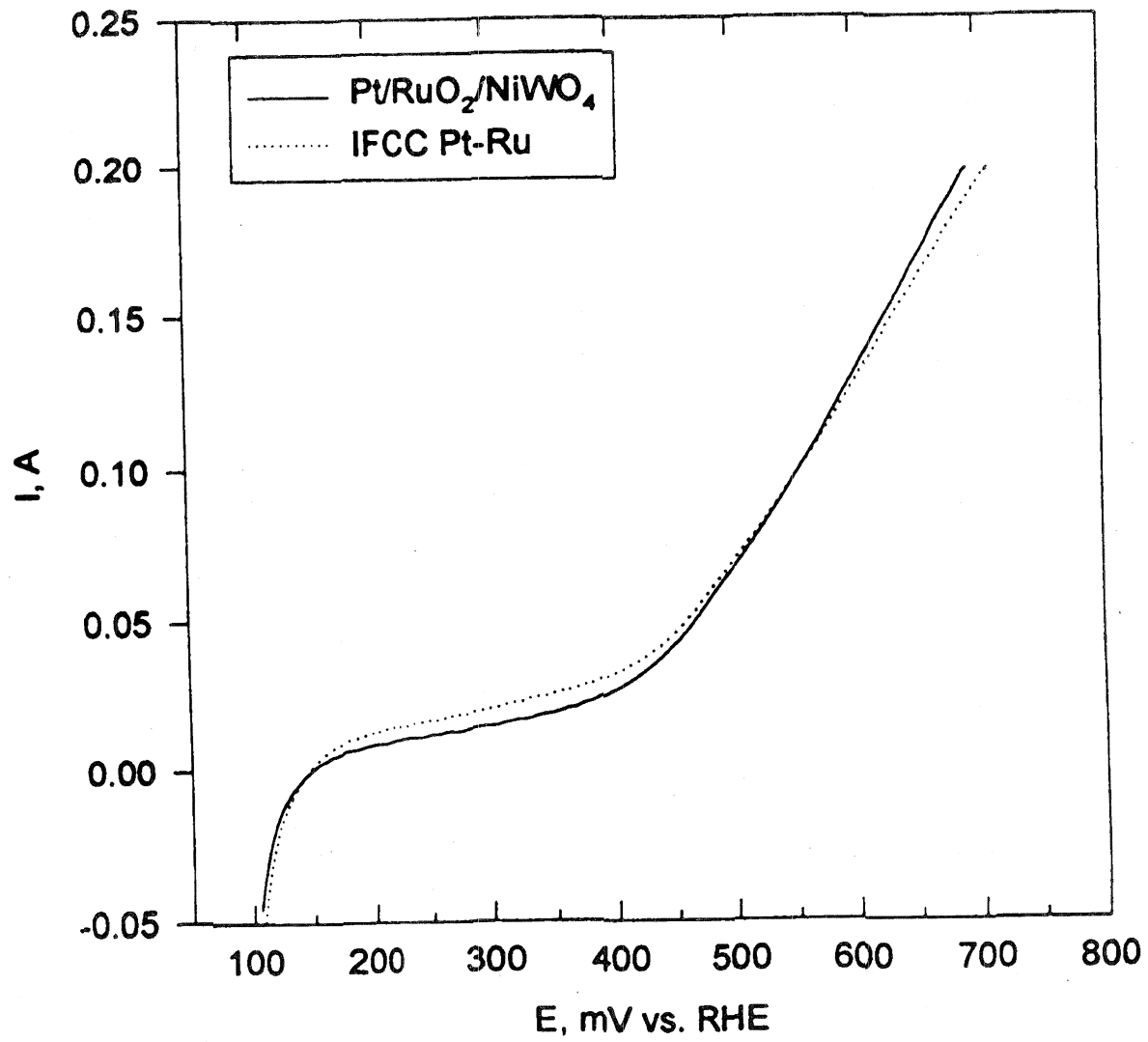Publications resulted from this project thus far:

1. N.S.Marinkovic, J.S.Marinkovic and R.R.Adzic, "*In situ* Infrared Spectroscopic Investigations of Sulfate Adsorption at Ag(111) Electrodes", *J.Electroanal.Chem.*, in press.

2. N.S.Marinkovic, J.X.Wang, J.S.Marinkovic and R.R.Adzic, "Unusual Adsorption Characteristics of Silver Adlayers on Pt(111) Electrode", *J.Phys.Chem.*, in press.

3. N.S.Marinkovic, J.X.Wang and R.R.Adzic, "In situ Spectroelectrochemical Investigation of CO Adsorption on Underpotentially Deposited Silver on Pt(111) Electrode", abstract No.1010, 193rd Meeting of the Electrochemical Society, San Diego, California, May 3-8, 1998.

4. R.R.Adzic and N.S.Marinkovic, "Bifunctional Electrocatalyst for Methanol Oxidation in Fuel Cells", patent pending.

5. S.Mukerjee, J.McBreen, N.S.Marinkovic and R.R.Adzic, "Comparative In Situ X-ray Absorption Studies of Pt-Ru and Pt-RuO$_2$ Electrocatalysts", in preparation.

6. N.S.Marinkovic and R.R.Adzic, "Methanol Oxidation on Pt/NiWO$_4$ and Pt/CoWO$_4$ Electrocatalysts", in preparation.

7. N.S.Marinkovic and R.R.Adzic, "In situ Spectroelectrochemical Investigation of Bisulfate and CO Adsorption on Ru(0001)", to be presented on 195th Meeting of the Electrochemical Society, Seatle, WA, May 2-7, 1999.
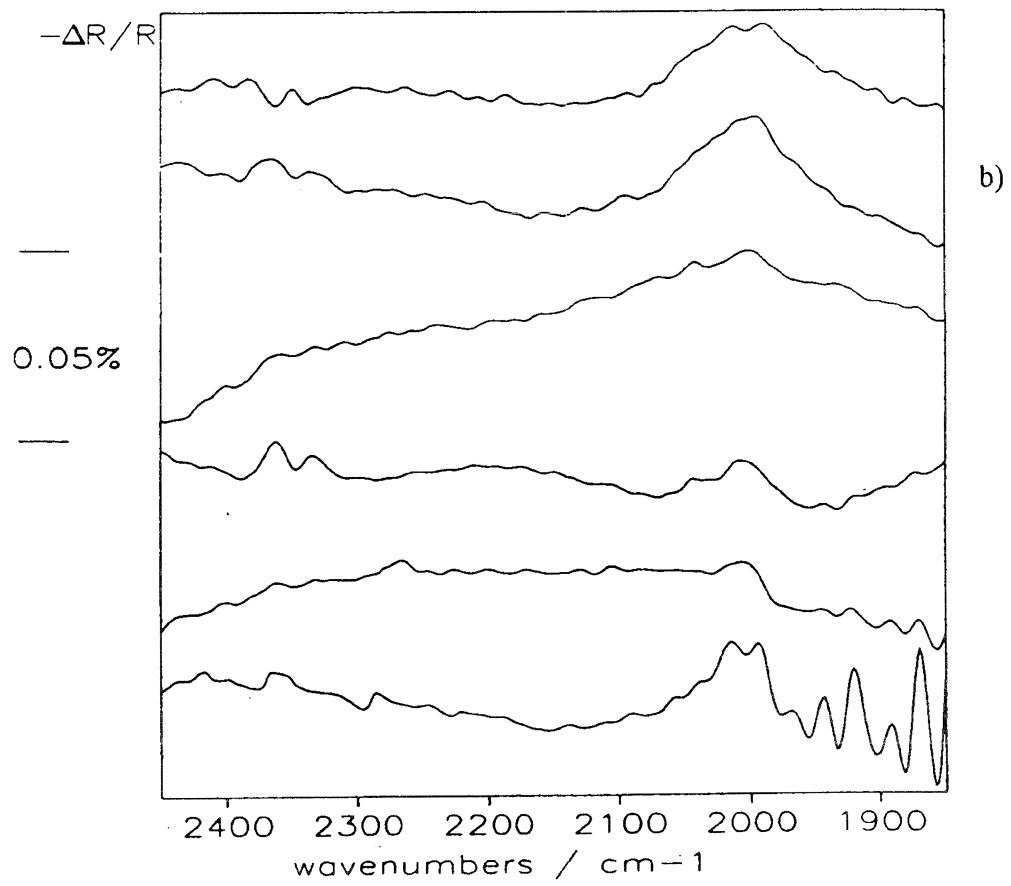
NiWO₄ in 0.5M H₂SO₄ + 0.5M CH₃OH

NiWO₄ in 0.5M H₂SO₄

a)

b)
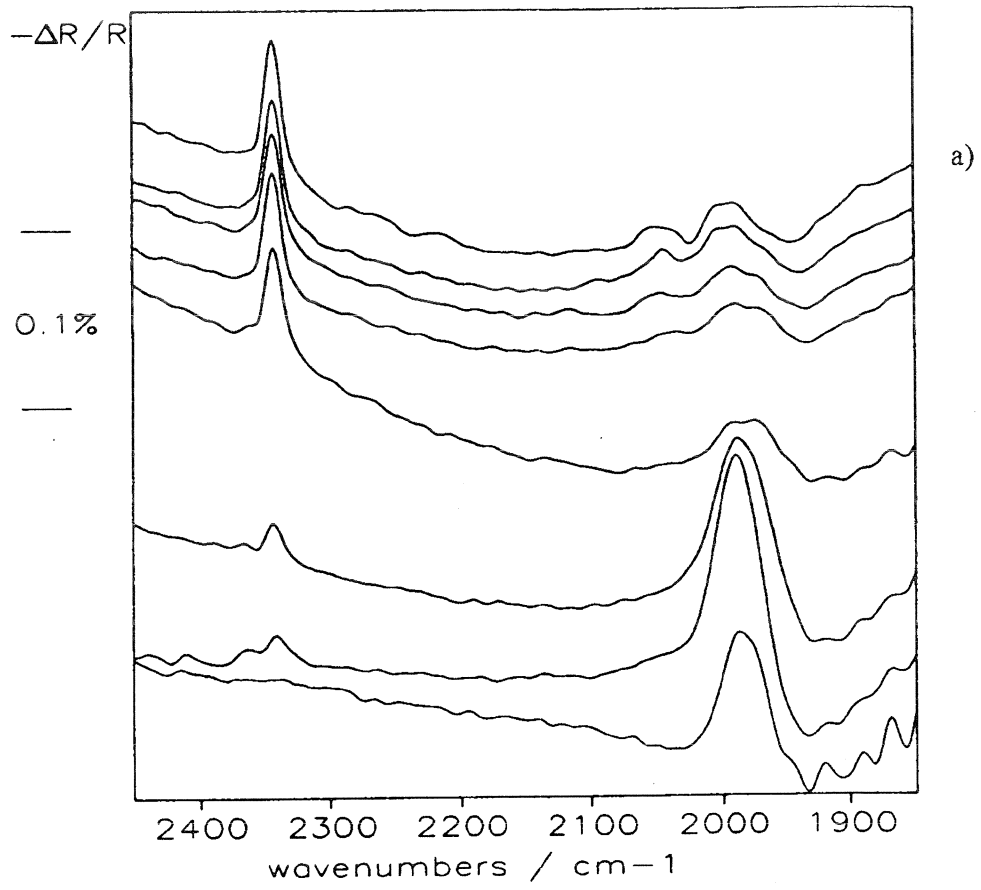
Fig. 4

In situ XANES for PtRu/C in 1 N HClO₄ + 0.3 N MeOH at the Ru K edge

Ru (black)
0.0 V vs RHE
0.54 V
0.70 V

Normalized Absorption

Energy relative to the Ru K edge (22117 eV)
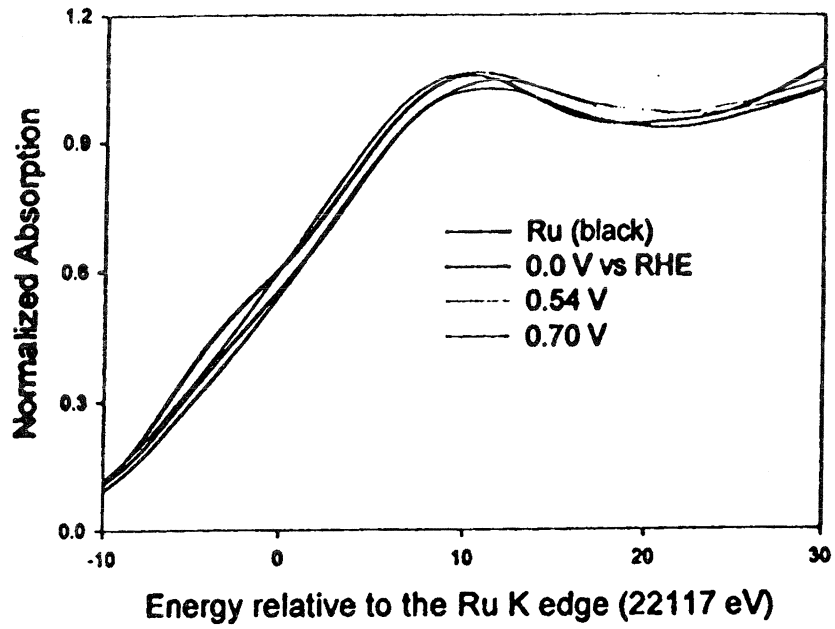
In situ XANES at the Ru K edge for Pt + RuO₂ sample in 1 N HClO₄ + 0.3 N MeOH

Ru black standard
Pt + RuOₓ at 0.0 V
0.54 V
0.70 V

Normalized Absorption

Energy Relative to the Ru K edge (22117 eV)
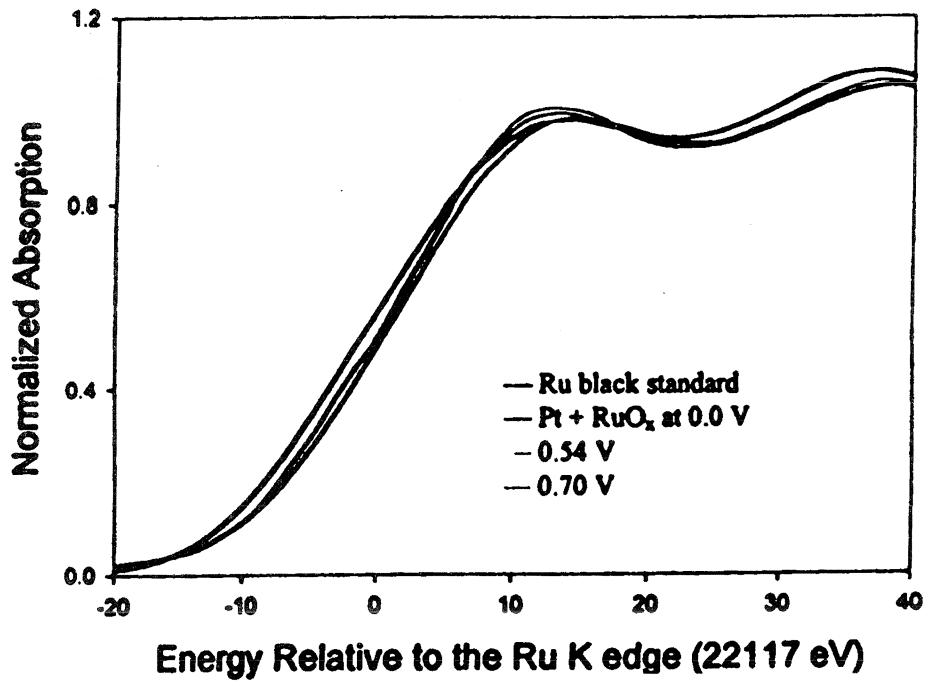
Appendix

Publications and manuscripts resulted thus far from this project.

In situ Infrared Spectroscopic Investigations of Sulfate Adsorption at the Ag(111) Electrode Surface[*]

N. S. Marinković, J. S. Marinković[*] and R. R. Adžić

Department of Applied Science, Brookhaven National Laboratory, Upton, NY 11973 and
[*]Department of Chemistry, University of California, Davis, CA 95616

Abstract

Cyclic voltammetry and *in situ* infrared spectroelectrochemistry were employed to study the ionic adsorption on the Ag(111) electrode surface in sulfate-containing solutions of different pH. It has been concluded that the sulfate anion is the predominant species adsorbed at the electrode surface in acidic and neutral medium. The adsorption of sulfate in alkaline solutions is inhibited by more strongly specifically adsorbed OH⁻ ions. The potential dependence of surface coverage, estimated on the basis of spectroelectrochemical data, indicates that a considerable repulsion exists among the adsorbed sulfate species. The spectral data were compared to that obtained for sulfate adsorption on Pt(111) and on underpotentially deposited Ag on the Pt(111) surface.

Keywords: FTIR spectroscopy; Adsorption; Sulfate; Silver(111) electrode

---

[*] Dedicated to Jean Clavilier on the occasion of his retirement from LEI CNRS and in recognition of his contribution to Interfacial Electrochemistry.

1. Introduction

Anion adsorption process on solid electrodes has been a topic of numerous investigations, mainly because it profoundly affects the kinetics of many electrochemical reactions. Recently, a number of *in situ* techniques has been utilized to study anion adsorption processes [1]. These studies include anion adsorption on Pt [2,3,4,5,6,7,8,9] and Au [10,11,12,13,14,15,16], using chronocoulometry [2,13], Fourier transform infrared (FTIR) [3-5,7,8,10-12], x-ray scattering [6,14,16], scanning tunneling microscopy (STM) [9,12], and radiotracer measurements [13], as well as surface enhanced Raman scattering (SERS) [17,18]. Unlike in the case of these two metals, adsorption data obtained by *in situ* techniques for silver electrodes are scarce.

In addition to extensive capacitance studies [19], radiotracer measurements conducted on polycrystalline [20,21] and, very recently, on single crystal surfaces [22] of silver provided quantitative information on a number of ions adsorbed, while STM [23] and x-ray scattering [16] furnished the structural information on the halide adlayer on Ag(111). The latter technique has been also utilized to study the water distribution at Ag(111)/electrolyte interface [24]. A recent visible-infrared sum-frequency generation (SFG) study provided a first determination of potential of zero charge of silver in CN⁻-containing NaClO₄ solution [25].

While all the above *in situ* techniques provide advantageous information on the structure of the metal/solution interface, only vibrational techniques, SERS and infrared-

based techniques, FTIR, SFG and second harmonic generation [26], can identify the type of the ion adsorbed. However, the inherent nature of the SERS technique, where a significant enhancement is achieved only after extensive roughening of the substrate, precludes the studies of well ordered single crystal surfaces. The aim of this work is to utilize the *in situ* FTIR spectroscopy to identify the nature of ions adsorbed on Ag(111). The data of sulfate and bisulfate adsorption at the Ag(111) electrode surface in three solutions of different pH presented here are compared to that of sulfate/bisulfate adsorption on Pt(111) and underpotentially deposited (UPD) silver on Pt(111) substrate [27,28].

2. Experimental

Silver single crystal electrode of 0.8 mm in diameter, obtained from Metal Crystals and Oxides, Cambridge Ltd. was oriented and cut to better than 0.5°, and mechanically polished with alumina and diamond pastes. Before each experimental run the crystal was polished by a procedure similar to the one described in Refs.[22] and [29], using a solution containing 50 ml of a 4M CrO_3 solution and 50 ml of a 0.6M HCl.

Reversible hydrogen electrodes (RHE) were used as the reference electrodes in acidic and neutral solutions, while Hg/HgO, 0.01M OH$^-$ served as the reference in alkaline medium. All reference electrodes were calibrated against a Ag/AgCl, 3M KCl electrode before and after each experiment. The electrode potentials throughout the text are given against this electrode. All chemicals were of the highest purity and used without

further purification. NaOH solutions were made from 50% w/w solution (Fisher) to eliminate possible carbonate contaminants. All solutions were made using MilliQ UV-plus water.

The *in situ* spectroelectrochemical measurements were conducted in a custom-made cell, described previously [7,30]. In this work, the CaF_2 hemispherical window was used and the optical path was modified accordingly. 90° off-axis mirrors, used in the external chamber of the Mattson RS-10000 to focus the IR light at the sample, were angled by 14° with respect to the horizontal plane so that the IR light was directed upward. The IR beam was focused at the CaF_2/solution interface and the incidence angle was set to 76° (Fig. 1). After the reflection from the interface, the IR light was collimated by a mirror and directed to the MCT detector. The spectrometer and a PAR 273 potentiostat were computer controlled using a program designed to set the potential of the working electrode alternatively to the sample or the reference potential for the working electrode prior to sample acquisition. The reference potential was constant and chosen to be near the onset of the hydrogen evolution in the supporting electrolyte. 4096 scans were coadded in cycles of 128 scans each; the resolution was 8 cm^{-1}. Spectra are given in the form of $-\Delta R/R$, with the positive-going bands representing a gain of a particular species at the sample potential relative to that at the reference.

The angle of incidence at 76° allows one to obtain information on the metal-adsorbate structure in a wide frequency range. Assuming that the refractive index of a dilute aqueous solution is close to that of water, one can draw a critical angle - frequency plot, Fig. 2. It is obvious that at the angle of incidence set to 76°, one obtains information in the whole frequency range from the cutoff of CaF_2 window (~1050 cm^{-1}) to better than

4000 cm^{-1}, with the exception of the regions where the refractive index of water becomes higher than that of the window, i.e. 1540 ~ 1620 and 2600 ~ 3340 cm^{-1}. The up-looking design of the spectroelectrochemical cell allows one for a quick check of the quality of the single crystal surfaces by recording voltammetry curves before and after the data collection.

3. Results and Discussion

3.1. Cyclic voltammetry

In order to explain the results obtained by SNIFTIRS in different media (*vide infra*), voltammograms of the Ag(111) in the corresponding solutions were recorded. Fig. 3a shows the voltammetry profile of the Ag(111) electrode in 0.01M NaOH. The shape of the voltammogram resembles that presented by Jović et al. [31] for neutral solutions, and differs from those of Savinova et al [32] and Droog [33] obtained in alkaline media. A characteristic "butterfly"-shaped peak is observed in the region -0.7 to -0.4 V. The curve in fact has the mirror-image similar to the famous Clavilier's butterfly [34] for hydrogen and bisulfate adsorption on Pt(111) in H$_2$SO$_4$ solutions.

In the recent work by Savinova et al. an overview of the earlier results and the assignments for the voltammetric features by different authors, involving hydrogen adsorption, underpotential deposition of Na$^+$ and chemisorption of hydroxide species have been reported [32]. However, correlating the peak to UPD of hydrogen is unlikely for

silver of any orientation, and the underpotential deposition of sodium cations in aqueous solution cannot be observed. Therefore, we conclude that the observed process should be correlated to the adsorption of hydroxide species with a considerable charge transfer, in agreement with the assignments by Savinova et al. [32]. The small spike at -0.7V probably represents some structural rearrangement of OH ions adsorbed on the Ag(111) surface. The adsorption process does not end at -0.4 V, as in the case of sulfate in neutral solution (Fig.3b), but continues with a similar charge transfer over a wide potential region up to -0.1V. A well defined peak is noticed in the voltammogram at the potentials positive of -0.1V. It probably corresponds to further oxidation of adsorbate which may lead to a formation of more discharged Ag-OH or Ag-O. At 0.1V a sharp spike is observed, indicating another structural arrangement of the ordered adsorbate. This is an unusual behavior for M-OH or M-O adsorbates which contrasts the behavior of disordered AuOH adlayer [35]. At more positive potentials the usually observed formation of Ag_2O is observed. When the potential is reversed, the same voltammetric features are observed in cathodic scan, i.e., all the processes are reversible.

In order to ascertain that chromate anions from polishing solutions are not affecting the shape of voltammetry curve, H_2 evolution was carried out during 1 min after the initial run was recorded. This procedure did not change the shape of the voltammogram, indicating the absence of adsorbed chromates at the electrode surface after the polishing procedure.

Figure 3b shows a set of cyclic voltammograms for the Ag(111) electrode in solutions of three different pH, viz. 0.05M H_2SO_4, 0.1M K_2SO_4 (pH ~ 7) and 0.1M K_2SO_4 + 0.1mM NaOH. Except for the curve in the acidic medium, where only the double layer

capacity charging is observed in the potential range limited by the hydrogen evolution and Ag dissolution on the negative and positive sides, respectively, the voltammograms for the neutral and alkaline media show pronounced peaks near the -0.6 V. Voltammograms similar to the one in Fig. 3a were presented earlier for the Ag(111) surface in neutral media of different anions [31]. Since the shape of the voltammogram depends somewhat on the nature of the anion in the supporting electrolyte, the authors concluded that the process represents the adsorption of the corresponding anion. However, our results indicate that the voltammetry features observed in neutral media should be correlated to those observed in alkaline solutions. As observed in Fig. 3, the addition of sulfate (up to 0.1M concentration) into 0.01M NaOH does not alter significantly the voltammetric profile. Therefore, the adsorption features in Fig. 3 for the Ag(111) electrode in neutral and alkaline sulfate solutions probably correspond to the identical processes which occur in the sulfate-free medium. However, sulfate ions affect the onset of AgOH or AgO formation in the alkaline medium by shifting it to more positive potentials, indicating a competitive adsorption of the two adsorbates. Similar process should be expected in the neutral medium. Therefore, the sulfate ions appear to be interacting strongly with the electrode surface, i.e., they are not only physisorbed as concluded in a recent Raman study [36]. It appears that the sulfate ions are chemisorbed as our FTIR results given below indicate. The fact that the voltammetry profiles presented in Fig. 3 show no Faradaic processes that could be correlated to sulfate adsorption is probably due to a small charge transfer from the sulfate ions to the surface.

3.2. SNIFTIRS measurements in 0.05M H₂SO₄

Fig. 4 shows SNIFTIR spectra obtained from sulfate adsorption on Ag(111) in 0.05M H_2SO_4. A distinctive feature of the spectra is a band at ~1170 cm^{-1} that shifts to the higher wavenumbers as the potential is made more anodic. Similar phenomenon has been reported for the bisulfate adsorption on Pt(111) in the same electrolyte [37]. A comparison of the spectra for the two metals, as well as for the sulfate adsorption on UPD Ag/Pt(111) substrate [27], however, reveals that there is a significant difference in frequencies of the bands. At the bare Pt(111) electrode and at a monolayer of silver deposited on Pt(111), the band for the sulfuric acid anions appears at ~1200 cm^{-1} and shifts to higher wavenumbers as the potential increases in anodic direction. This shift has a rate of ~100 and ~40 cm^{-1}/V for Pt(111) and monolayer of Ag on Pt(111), respectively [38,27]. At Pt(111), this band was ascribed to the strongly blue-shifted SO_3 stretch of adsorbed bisulfate on platinum surface, or, more precisely, to the H_3O^--SO_4^{2-} ion pair. It has also been shown that the band is only seen when the solution pH is close to, or below the pKa for the sulfate/bisulfate conversion, i.e. in solutions of pH lower than 2.0. It is absent in solutions of higher pH values [37].

In the IR frequency region above 1000 cm^{-1}, HSO_4^- anion in an aqueous solution shows an antisymmetric stretching mode of SO_3 at 1195 cm^{-1}, and a totally symmetric stretch at 1040 cm^{-1}. The latter band could not be observed in the present experiments due to proximity to the cutoff of the window used. A single band is observed for a sulfate-

containing aqueous solution at 1104 cm^{-1}, representing the antisymmetric stretching mode of the SO_4^{2-} anion [39].

The band at ~1170 cm^{-1} in Fig. 4, therefore, could be ascribed either to red-shifted $v_{as}(SO_3)$ for bisulfate ion, or strongly blue shifted bands for bisulfate and sulfate species. A shift to lower wavenumbers (to the red) physically represents a weakening of the S=O bonds in a bisulfate molecule. *Ab-initio* calculations show that oxygen lone-pair electron orbitals exhibit anti-bonding character for SO bond in bisulfate and that the donation of these lone-pair electrons to metal surface should cause strengthening of the SO bond [8]. Upon approach of a positively charged species (Li$^+$ in [8]), the authors showed that the $v_s(SO_3)$ mode shifts to higher, and the $v_{as}(SO_3)$ mode to lower frequencies. With increasing positive charge of the approaching species, however, the $v_{as}(SO_3)$ mode should be moved further to the red. In the present case, the band at ~1170 cm^{-1} in Fig. 4 moves to higher frequencies as the potential is made more positive. Therefore, ascribing the band at ~1170 cm^{-1} to the $v_{as}(SO_3)$ mode of bisulfate would be difficult to justify.

In order to find the further information on the predominant species adsorbed on the metal surface, the study has been conducted in the solutions of different pH values. As it will be presented below, the band at ~1170 cm^{-1} appears in acidic solutions of pH both below and above the second dissociation constant of sulfuric acid (pK$_a$=1.93). Since the concentration of bisulfate ions in a neutral solution is negligible, the band is ascribed to the strongly shifted $v(SO_4^{2-})$ mode of sulfate. This judgment is also supported by the data of Shi et al. who, on the basis of chronocoulometric and radiotracer measurements, concluded that sulfate is the predominant species adsorbed on Au, another metal of similar electronic structure, even at low pH values [10]. Furthermore, a Raman study of

polycrystalline silver in 1M H_2SO_4 shows no signs of the bands for the adsorbed HSO_4^- ions [40]. A broad band at 1165 cm^{-1} observed in that study was correlated to sulfate adsorbed on the Ag electrode. On the other hand, the conclusion on the predominant sulfate adsorption on Ag(111) is in apparent disagreement with that of Horanyi et al. [20]. The authors concluded that bisulfate should be the predominant adsorbed species at a polycrystalline silver electrode, although it has been acknowledged that the strong electric field in the double layer near the silver electrode may facilitate the dissociation of bisulfate ions therein [20,21].

The potential dependency of the integrated area of the electrode for two separate runs is given in Fig. 5a. It is calculated as the area under the baseline-corrected band in the region $v_p \pm 25$ cm^{-1}, where v_p is the peak frequency, and normalized with the instrument throughput factor for each experimental run. This factor is considered to be constant within an experiment, and represents the figure of merit for the IR spectroelectrochemical experiment, as discussed in Ref. [7]. The pseudo-isotherms given in Figure 5a are consistent with electrochemical and radiotracer investigations of bisulfate-anion adsorption on Ag [19-22]. The amount of anion adsorbed on the metal surface monotonically increases up to 0.2 V. However, as the potential is further increased, it seems that the anion coverage reaches a saturation indicated by a plateau above 0.25 V.

The pseudo-isotherm in Fig. 5a with a linear dependence of coverage in a relatively wide potential region indicates a Temkin adsorption behavior, i.e. a repulsive interaction among sulfate anions at the Ag(111) electrode. The repulsive interaction is in agreement with the results of Smolinski et al. [22] who found that the Frumkin adsorption behavior with repulsion between adsorbate species for Ag(111) and that only 34% of the electrode

surface is covered with sulfate. However, our voltammetry curves (*vide supra*) together with the FTIR results presented in the next section indicate that the sulfate coverage could be even smaller.

Figure 5b shows the peak frequency of the adsorbed sulfate band as a function of the applied potential. A linear dependence is obtained in the wide range of the potential, with a slope of about 60 cm^{-1}/V. A close observation of the Fig. 5b shows that the slope can be as high as 110 cm^{-1}/V in the potential range up to about 0.1 V vs. Ag/AgCl. A comparison of the data presented in Figs. 5a and 5b reveals that the slope may depend on the coverage of the sulfate at the surface, as discussed in the next paragraph.

The frequency shift with potential of the species adsorbed on electrode surfaces can be explained in terms of one or more of the following mechanisms: electron donation between the adsorbate and the metal surface (vibronic coupling), coupling of the electric field that exist in the double layer with the dipole moment of the adsorbates (Stark effect), and interaction from dipole-dipole coupling due to coverage increase [41,42]. It is possible that the last mechanism lowers the v_p (E) slope in Fig. 5b at the higher coverages. Furthermore, the large interactive parameter for sulfate at Ag(111) [22] indicates a small charge transfer from the adsorbed sulfate ions to the electrode surface, in the agreement with the shape of the cyclic voltammograms in Fig.3, where no process other than the double layer charging is observed. Consequently, a large repulsion exist among the partially negative-charged adsorbates, which could cause the lowering of the peak frequency plot with the potential in Fig. 5b.

3.3. SNIFTIRS measurements in 0.1M K₂SO₄.

Fig. 6 shows SNIFTIRS spectra of anion adsorption on the Ag(111) surface in 0.1M K_2SO_4. As in the previous section, a strong, positive going band at ~1160 cm^{-1} is observed. The peak maximum of the band steadily shifts to higher wavenumbers as the potential is made more positive. Since the concentration of bisulfate ions is negligible in the neutral solution, the band is associated with the adsorption of sulfate species at the silver surface.

The reference spectrum for the spectra presented in Fig. 6 is taken at -0.48V, i.e. in the range of AgOH formation. As can be inferred from the voltammogram in Fig. 3, the AgOH formation proceeds all the way to about -0.2V. On the other hand, since the SNIFTIRS bands become visible in spectra above -0.33 V, one concludes that SO_4^{2-} ions adsorb at the surface partially occupied by hydroxyl anions.

The SNIFITRS band corresponding to the sulfate adsorption at 1160 cm^{-1} increase in intensity up to about 0.02V. As seen from the Fig. 6, the three topmost spectra taken at potentials of 0.02 and above have practically identical intensity. This behavior can be seen more clearly in the Fig. 7a, where the integrated band intensities for two separate runs are plotted as a function of potential of the Ag(111) electrode. The A_i (E) plot in Fig. 7a shows that a plateau is reached above 0.02V.

Fig. 7b shows the frequency change of the band for adsorbed sulfate with potential in 0.1M K_2SO_4. A potential shift of the band maximum with a rate of 40 cm^{-1}/V is observed in the entire potential region. Such a relatively small shift, as well as the absence

of the change in the v_p (E) plot, as opposed to those observed in the acidic medium indicate that adsorption processes take place in different chemical environment in the two solutions. The most probable reason for this is the competition for sites between adsorbed OH and SO_4^{2-} ions in the neutral medium. The sulfate adsorption in the acidic solution proceeds on the silver electrode free of anions, whereas that in the neutral medium advances on an electrode partially occupied by hydroxyl groups. From the differences in sulfate concentration in acidic and neutral media one could expect that the SNIFTIR spectra taken in the neutral solution should have higher intensity. The differences in the chemical environment, which lead to a different surface state, make the sulfate bands in the neutral solution to be less intense.

3.4. SNIFTIRS measurements in 0.5M H_2SO_4 and in 0.1M K_2SO_4 + 0.01M NaOH

Spectra for the sulfate adsorption in the highly concentrated sulfuric acid solution are given in Fig. 8. The sulfate band at ~1170 cm^{-1} is observed again, as in the two previous solutions discussed above, but with a much smaller intensity. In fact, the band could be distinguished from the background noise only in the spectra taken at the most positive potentials. This is not surprising, since in this solution the sulfate concentration is about 40 times smaller than that of bisulfate.

It has been assumed that a strong electric field near the polycrystalline silver electrode may facilitate the conversion of bisulfate into sulfate ions [20,21]. If such a process is operative in the case of the Ag(111) / 0.5M H_2SO_4 system, the loss of bisulfate

in the double layer should be observed in a SNIFTIR spectrum as a negative-going band centered at ~1200 cm^{-1}, which gains in intensity as the potential is made more positive. No such band is seen in Fig. 8. Consequently, the intensity of the sulfate band at ~1170 cm^{-1} is governed solely by the bulk concentration of sulfate in this solution. If one assumes a negligible ion diffusion from the bulk of the solution into the solution gap between the electrode and the window, and the gap thickness of 1 μm, one obtains the maximum surface coverage of sulfate to be about θ = 0.30, taking the nearest neighbor separation for silver of 0.2889 nm [43] and the bulk SO_4^{2-} concentration of 12 mM. This value is close to the maximum coverage of sulfate at Ag(111) calculated on the basis of radiotracer measurements [22]. The intensity of the bands in Fig. 8 is, however, too small for such a large coverage of SO_4^{2-}. The sulfate coverage of θ = 0.3 is close to a completely covered Ag(111) surface with ions adsorbed on three-fold symmetry sites. Such adsorption requires a considerable charge transfer which would produce a small peak in voltammetry curve, similar to that at Pt(111). This is not observed for Ag(111), see Fig. 3. Therefore the FTIR and voltammetry data indicate that the sulfate coverage on Ag(111) is small.

From the three topmost spectra in Fig. 8 one can estimate the rate of the shift of the sulfate adsorption band with the potential to be about 50 cm^{-1}/V. However, due to low intensity of the bands, the plots of v_p (E) and A_i (E) are not given here.

In the solution of 0.1M K_2SO_4 + 0.01M NaOH the sulfate bands in the SNIFTIR spectra could not be distinguished from the background. We therefore conclude that the OH ions, which are known to be more specifically adsorbed than sulfate, preclude the adsorption of SO_4^{2-}. From the voltammogram in Fig. 3 one observes that the adsorption of hydroxyl ions and formation of AgOH proceeds all the way to the onset of silver

oxidation. The fractional coverage of hydroxyl groups increases with the potential, leaving less free sites for the sulfate adsorption. This is different from the behavior in the neutral solution where in the potential region between -0.2 and 0.2 V no process other than the double layer charging is observed in the voltammogram so that the sulfate adsorption can proceed on the sites free of OH⁻ ions.

4. General Discussion and Conclusions

The adsorption of sulfuric acid anions on Ag(111) is interesting to compare with adsorption on Ag monolayer and bilayer on the Pt(111) electrode surface. A comparison of the spectra for these three surfaces reveals significant differences in adsorption properties. It has been found that the bisulfate ions strongly adsorb on the Pt(111) surface [37,38], while sulfate species are predominantly adsorbed on Ag(111) surface, as shown in the present work. On the Ag monolayer on Pt(111), however, the adsorption of bisulfate is observed [27]. This indicates that Pt strongly affects the electronic properties of Ag monolayer. Adsorption of CO on this surface [44], but not on Ag(111), corroborates the above view, as well as redistribution of charges in 5d- and 4d-orbitals of Pt and Ag observed at metal-gas interface [45]. On the Ag bilayer on Pt(111), adsorption of sulfate is observed [27] as on the bulk Ag(111), indicating that already the Ag bilayer on Pt(111) acquires some of the bulk Ag properties. These data suggest an interesting correlation between the adsorption behavior and the chemical nature of the metal surface. It appears that the (111) oriented surfaces of sp-metals, like Ag and Au [13], predominantly adsorb

sulfate anions, whereas a d-metal Pt adsorb bisulfate. It remains to be seen whether this conclusion can be applied to other d-metals.

In summary, the data obtained by *in situ* spectroelectrochemistry presented above demonstrate specific adsorption of sulfate anions on the Ag(111) electrode surface. Pseudo-isotherms obtained from IR data show a large lateral repulsion between adsorbed sulfate anions indicating a small charge transfer in this system. Voltammetric and FTIR data indicate that the strong specific adsorption of hydroxyl anions on Ag(111) in solutions of higher pH values inhibit the adsorption of sulfate, eventually completely blocking it in strong alkaline solutions.

Acknowledgments

References

[1] *Electrochemical Interfaces*, H.D.Abruña (Ed.), VCH Publishers, New York (1991).

[2] W.Savich, S.G.Sun, J.Lipkowski and A.Wieckowski, *J.Electroanal.Chem.*, **388** (1995) 233.

[3] C.S.Kim and C.Korzeniewski, *J.Phys.Chem.*, **97** (1993) 9784.

[4] E.Pastor, A.Rodes and T.Iwasita, *J.Electroanal.Chem.*, **404** (1996) 61.

[5] K.Ashley, D.L.Feldheim, D.B.Parry, M.G.Samant and M.R.Philpott, *J.Electroanal.Chem.*, **373** (1994) 201.

[6] C.A.Lucas, N.M.Marković and P.N.Ross, *Phys.Rev. B*, **55** (1997) 7964.

[7] P.W.Faguy and N.S.Marinković, *Anal.Chem.*, **67** (1995) 2791.

[8] Y.Sawatari, J.Inukai and M.Ito, *J.Electron Spec.Rel.Phenomena*, **64/65** (1993) 515.

[9] A.M.Futnikov, U.Stimming and R.Vogel, *J.Electroanal.Chem.*, **428** (1997) 147.

[10] M.C.P.M.da Cunha, M.Weber and N.C.Nart, *J.Electroanal.Chem.*, **414** (1996) 163.

[11] M.Weber and N.C.Nart, *Electrochim.Acta*, **41** (1996) 653.

[12] G.Edens, X.Gao and M.J.Weaver, *J.Electroanal.Chem.*, **375** (1994) 357.

[13] Z.Shi, J.Lipkowski, M.Gamboa, P.Zelenay and A.Wieckowski, *J.Electroanal.Chem.*, **366** (1994) 317.

[14] O.M.Magnussen, B.M.Ocko, R.R. Adžić and J.X.Wang, *Phys.Rev. B*, **51** (1995) 5510.

[15] J.X.Wang, G.M.Watson and B.M.Ocko, *J.Phys.Chem.*, **100** (1996) 6672.

[16] B.M.Ocko, O.M.Magnussen, J.X.Wang, R.R. Adžić and Th.Wandlowski, *Physica B*, **221** (1996) 238.

[17] M.Fleischmann, P.Graves, I.Hill, A.Oliver and J.Robinson, *J.Electroanal.Chem.*, **150** (1983) 33.

[18] T.Itoh, Y.Sasaki, T.Maeda and C.Horie, *Surf.Sci.*, **389** (1997) 212.

[19] A.Hamelin, *J.Electroanal.Chem.*, **145** (1983) 225.

[20] G.Horanyi, E.M.Rizmayer and J.Konya, *J.Electroanal.Chem.*, **176** (1984) 339.

[21] P.Zelenay, M.Gamboa-Aldeco, G.Horanyi and A.Wieckowski, *J.Electroanal.Chem.*, **357** (1993) 307.

[22] S.Smolinski, P.Zelenay and J.Sobkowski, *J.Electroanal.Chem.*, **442** (1998) 41.

[23] G.Aloisi, A.M.Futnikov and T.Will, *J.Electroanal.Chem.*, **370** (1994) 297.

[24] M.F.Toney, J.N.Howard, J.Richer, G.L.Borges, J.G.Gordon, O.R.Melroy, D.G.Wiesler, D.Yee and L.B.Sorensen, *Surf.Sci.*, **335** (1995) 326.

[25] A.Tadjeddine, A.Permans and P.Guyot-Sionnest, *Surf.Sci.*, **335** (1995) 210.

[26] F.T.Wagner and P.N.Ross Jr., *J.Electroanal.Chem.*, **150** (1983) 141.

[27] N.S.Marinković, J.S.Marinković and R.R.Adžić, in preparation.

[28] N.S.Marinković, J.X.Wang and R.R.Adžić, Proceedings of the Electrochemical Society, Vol.97-17, Pennington, NJ (1997), p.251.

[29] A.Hamelin, L.Doubova, L.Stoicoviciu and S.Trasatti, *J.Electroanal.Chem.*, **244** (1988) 133; T.Kurasawa, Patent, Japan, 35-5619, May 23, 1960.

[30] N.S.Marinković, M.Hecht, J.S.Loring and W.R.Fawcett, *Electrochim.Acta*, **41** (1996) 641.

[31] V.D.Jović, R.Parsons and B.M.Jović, *J.Electroanal.Chem.*, **339** (1992) 327.

[32] E.R.Savinova, P.Kraft, B.Pettinger and K.Doblhofer, *J.Electroanal.Chem.*, **430** (1997) 47.

[33] J.M.M.Droog, *J.Electroanal.Chem.*, **115** (1980) 225.

[34] J.Clavilier, R.Faure, G.Guinett and R.Durand, *J.Electroanal.Chem.*, **107** (1980) 205.

[35] C.M.Vitus and A.J.Davenport, *J.Electrochem.Soc.*, **141** (1994) 1291.

[36] L.Rintoul, K.Crawford, H.F.Shurvell and P.M.Fredericks, *Vibrational Spectrosc.*, **15** (1997) 171.

[37] P.W.Faguy, N.S.Marinković and R.R.Adžić, *Langmuir*, **12** (1996) 243.

[38] P.W.Faguy, N.S.Marinković and R.R.Adžić, *J.Electroanal.Chem.*, **407** (1996) 209.

[39] S.D.Ross, *Inorganic Infrared and Raman Spectra*, McGraw Hill, London, 1972.

[40] Y.Sasaki and Y.Nishina, *Surf.Sci.*, **242** (1991) 549.

[41] R.M.Hammaker, A.Francis and R.P.Eischens, *Spectrochim.Acta*, **21** (1965) 1295.

[42] K.Ashley and S.Pons, *Chem.Rev.*, **88** (1988) 673.

[43] J.X.Wang, N.S.Marinković, R.R.Adzić and B.M.Ocko, *Surf.Sci.Letters*, **398** (1998) L291.

[44] N.S.Marinković, J.X.Wang and R.R. Adžić, 193rd Meeting of Electrochemical Society, San Diego, CA, May 03-08 1998, abstract No.1010.

[45] J.A.Rodriguez and M.Kuhn, *J.Phys.Chem.*, **98** (1994) 11251.

Figure Captions

Figure 1. The optical path of the spectroelectrochemical cell used in the study. A, A', 90°
off-axis mirrors; B, CaF_2 hemisphere; C, Teflon cell body; D, Silver electrode;
E, Teflon tube; F, Pt wire; G, IR source; and H, MCT detector. The counter
electrode (Pt wire wound in a loop around the working electrode) and the
reference electrode, pushed from a side into the Teflon cell body were omitted
from the drawing for clarity.

Figure 2. Critical angle dependency on frequency for the CaF_2 / water interface. Dotted
line represents the angle of incidence of 76°, used in this study.

Figure 3. Voltammetry curves for the Ag(111) electrode in 0.01M NaOH (a), and in
sulfate-containing solutions of different pH (b): 0.05M H_2SO_4 ($- \cdot - \cdot$), 0.1M
K_2SO_4 (- - - -) and 0.1M K_2SO_4 + 0.01M NaOH (———). Sweep rate 50
mV/s.

Figure 4. SNIFTIR spectra of sulfate adsorption on Ag(111) in 0.05M H_2SO_4. 4096 scans
were coadded in 16 cycles, 256 scans each; the resolution was 8 cm^{-1}. Spectra
are collected in the potential range from -0.193 (bottom spectrum) to 0.307 V
vs. Ag/AgCl, 3M KCl (top spectrum) in 45 mV increments. Reference spectra
obtained at -0.223 V. Spectra are offset for clarity.

Figure 5. Integrated intensity (a), and peak maxima (b) dependency on potential of the
working electrode for two independent measurements of Ag(111) in 0.05M
H_2SO_4, normalized by the throughput factor.

Figure 6. SNIFTIR spectra of sulfate adsorption on Ag(111) in 0.1M K_2SO_4. Sample
spectra are collected in the potential range from -0.38 (bottom spectrum) to
0.12 V vs. Ag/AgCl, 3M KCl (top spectrum) in 50 mV increments. 4096 scans
were coadded in 16 cycles, 256 scans each; the resolution was 8 cm^{-1}.
Reference spectra obtained at -0.48 V. Spectra are offset for clarity.

Figure 7. Integrated intensity (a), and peak maxima (b) dependency on potential of the
working electrode for two independent measurements of Ag(111) in 0.1M
K_2SO_4, normalized by the throughput factor.

Figure 8. SNIFTIR spectra of sulfate adsorption on Ag(111) in 0.5M H_2SO_4. Sample
spectra are collected in the potential range from -0.125 (bottom spectrum) to
0.275 V vs. Ag/AgCl, 3M KCl (top spectrum) in 50 mV increments. 4096
scans were coadded in 16 cycles, 256 scans each; the resolution was 8 cm^{-1}.
Reference spectra obtained at -0.225 V. Spectra are offset for clarity.
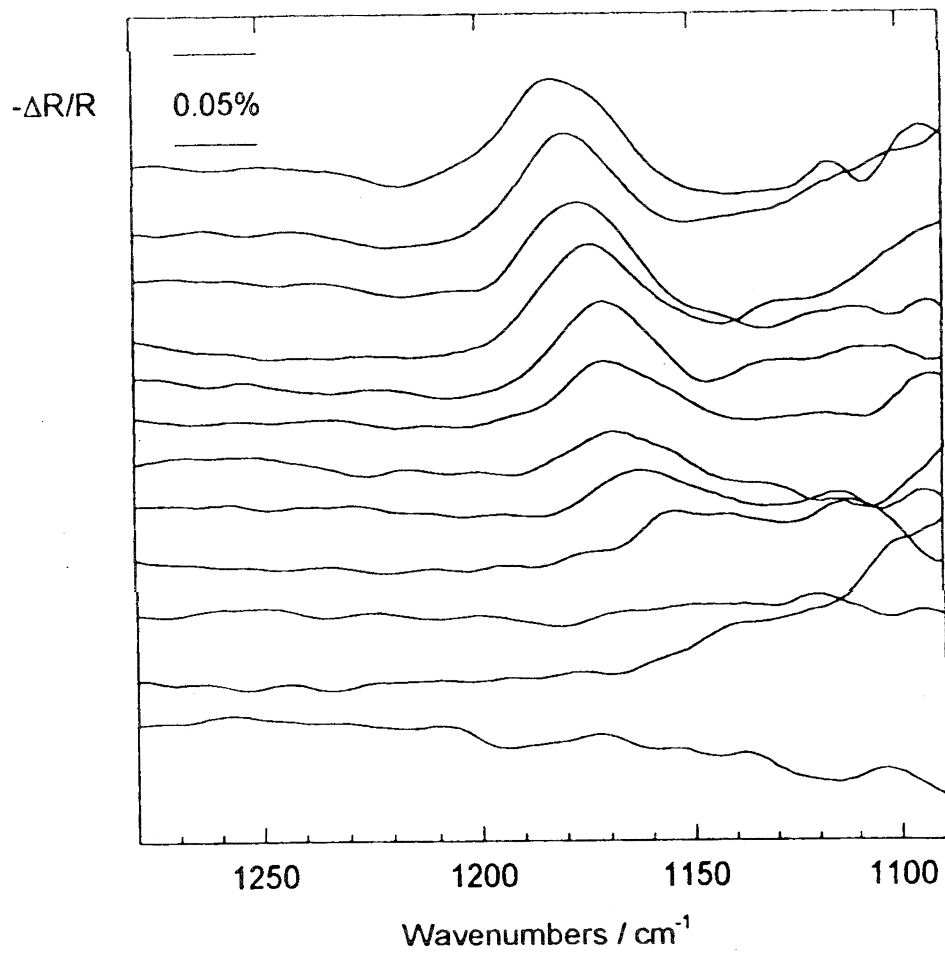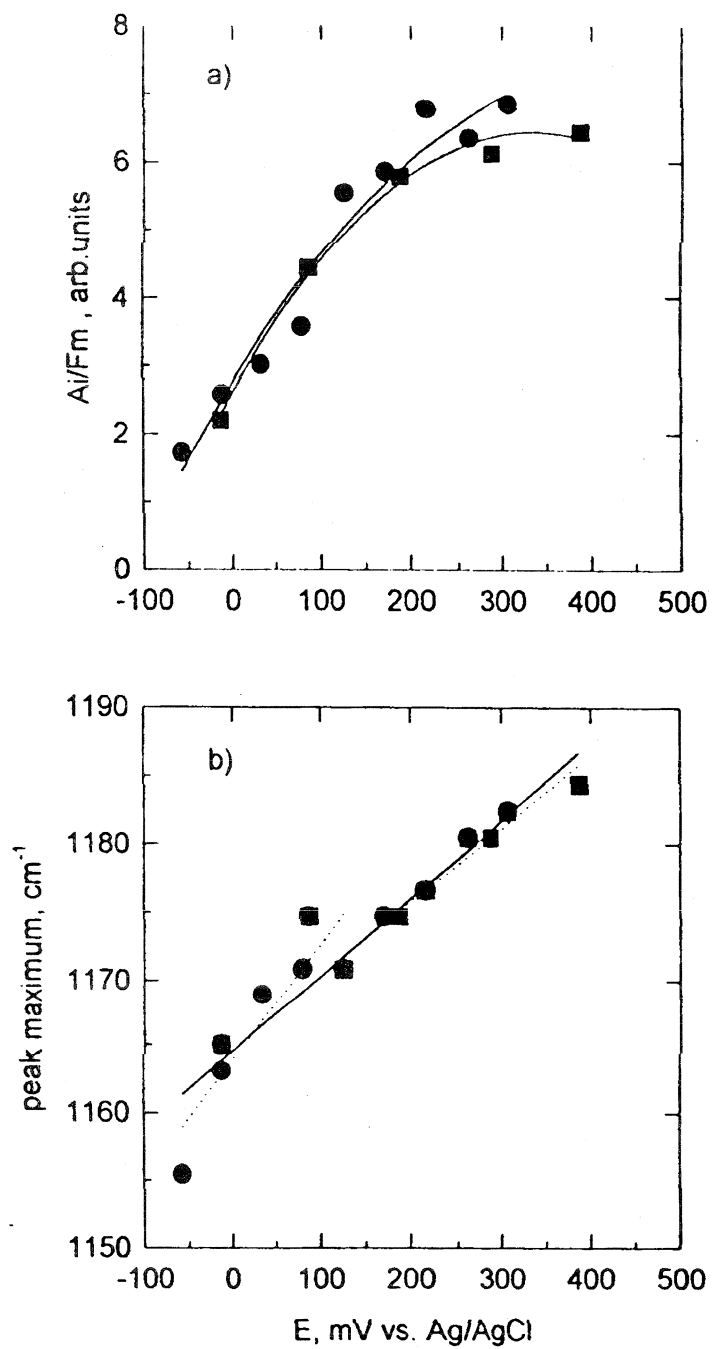
F

G

E

C

D

B

H

A

A'
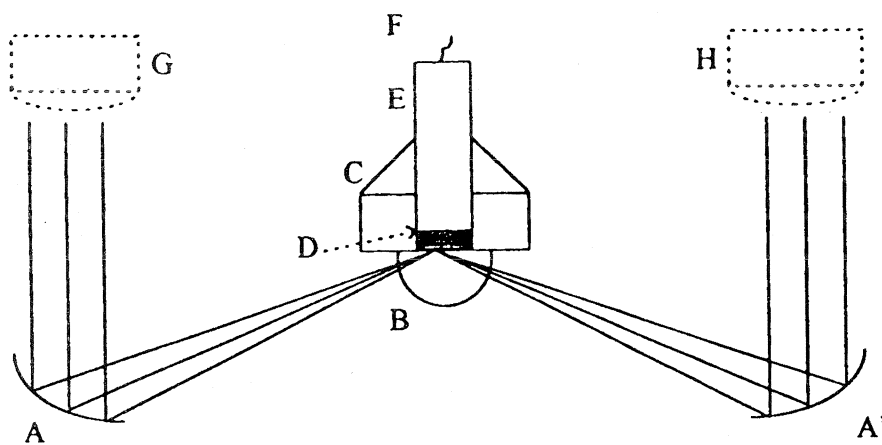
N.S.Marinkovic et al., "In situ Infrared Spectroscopic Investigations...", Figure 1.
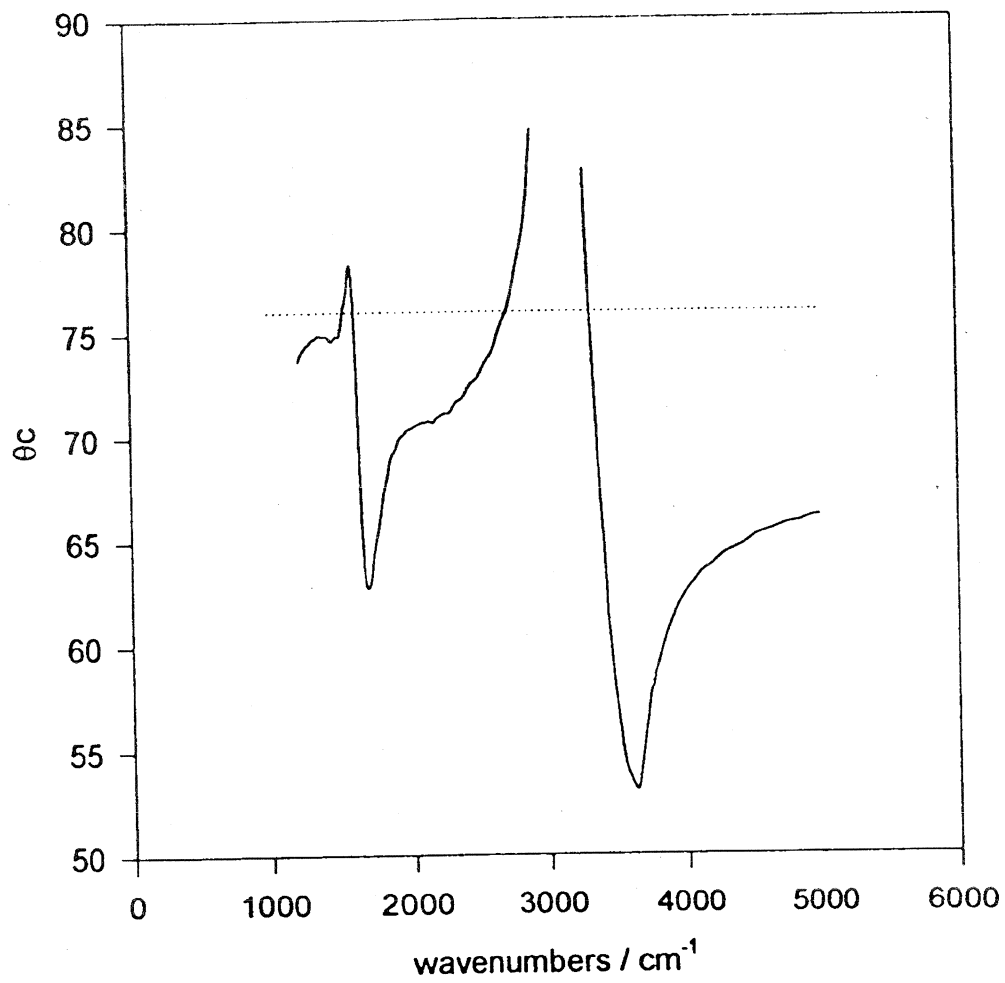
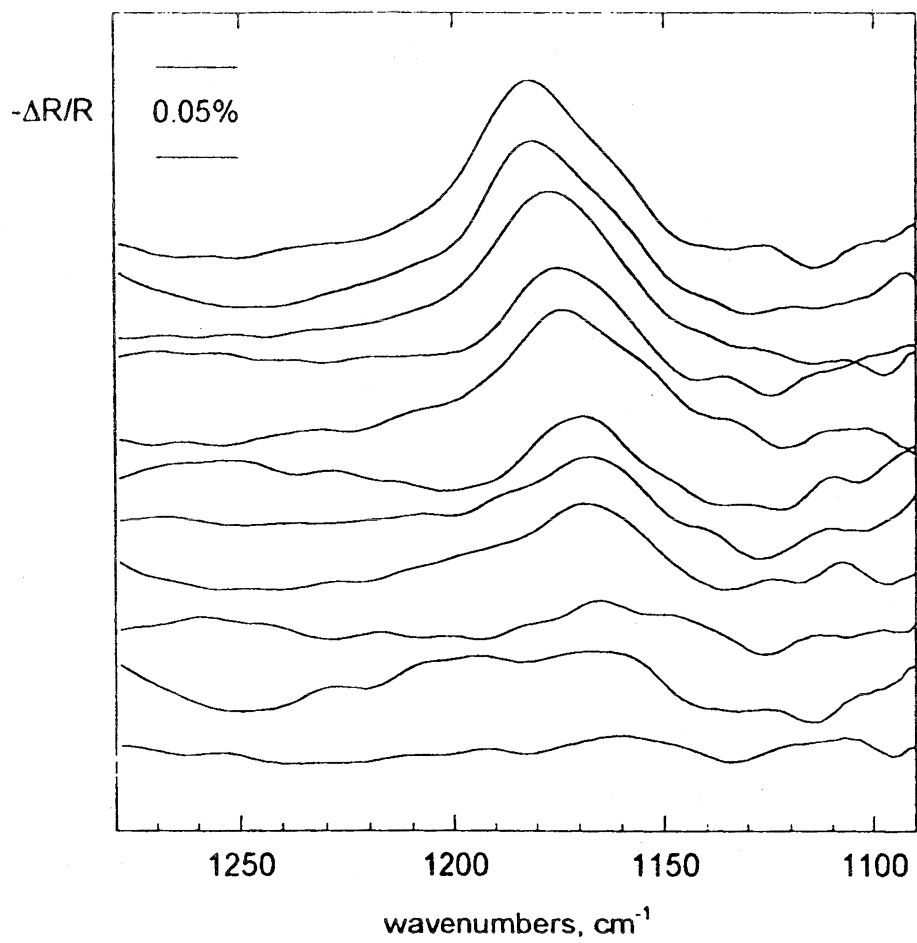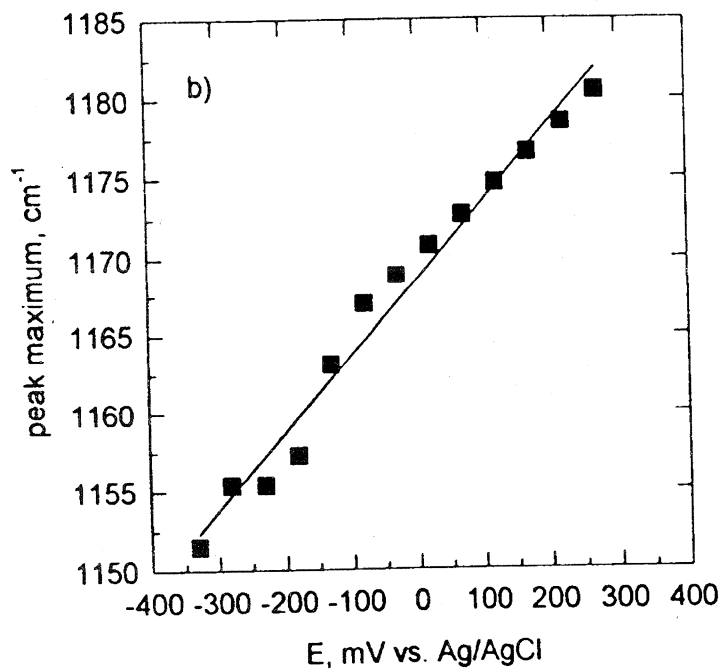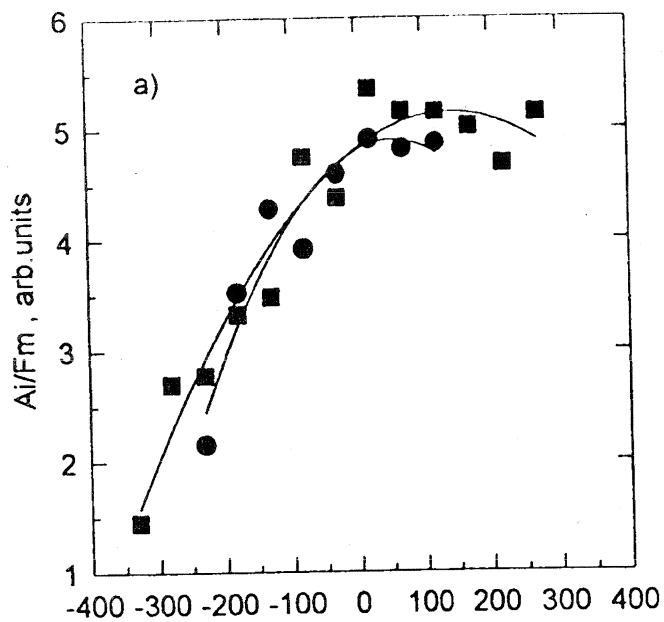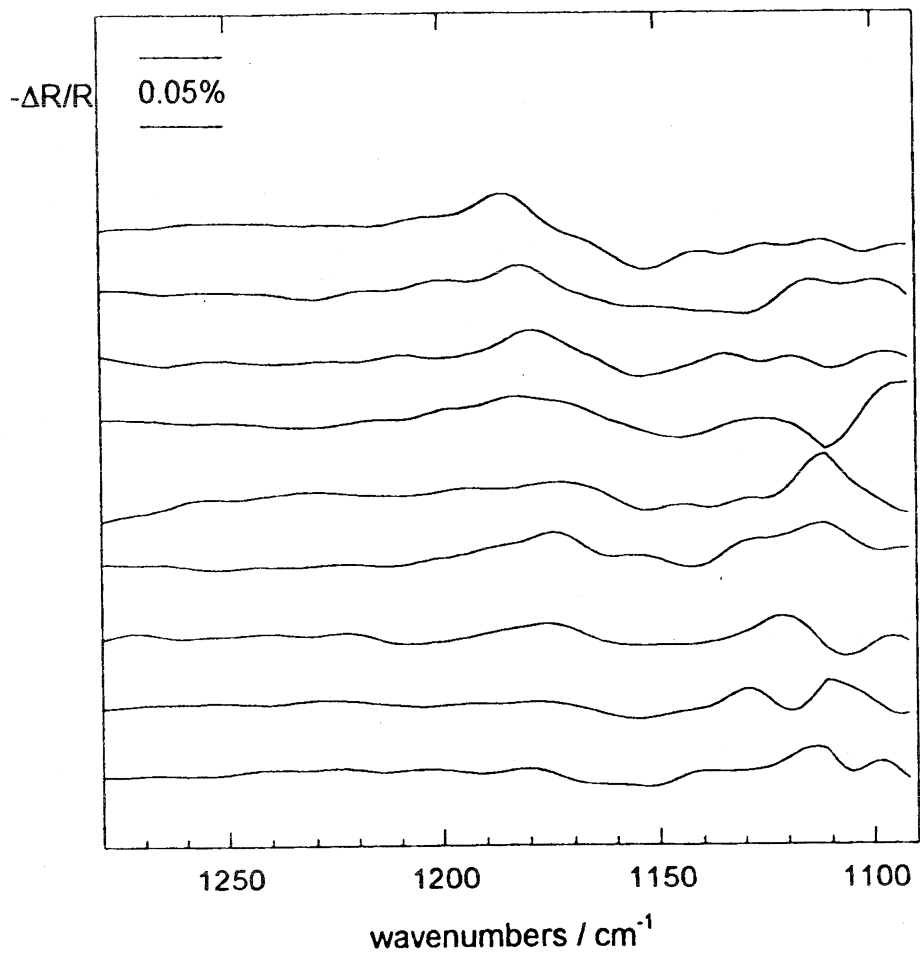N.S.Marinkovic et al., "In situ Infrared Spectroscopic Investigations...", Figure 2.

a)

b)
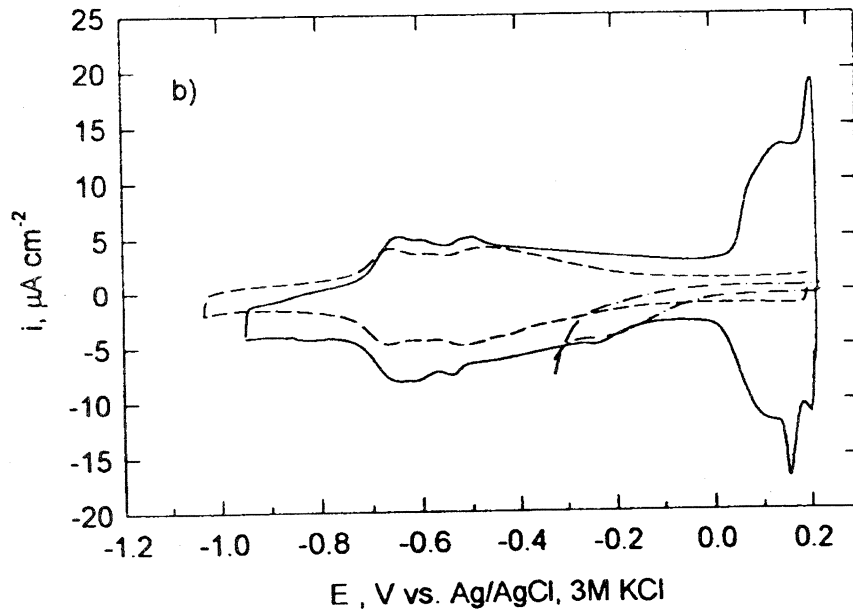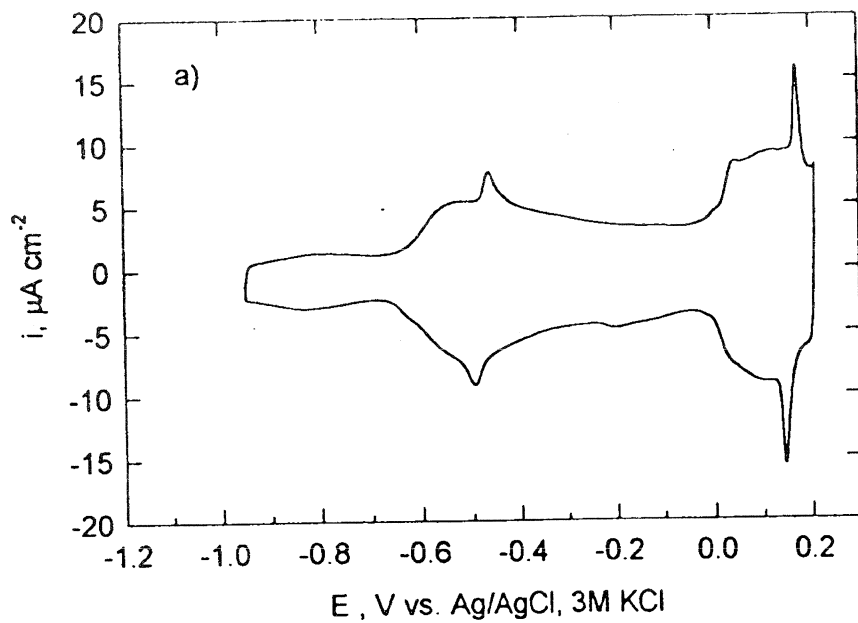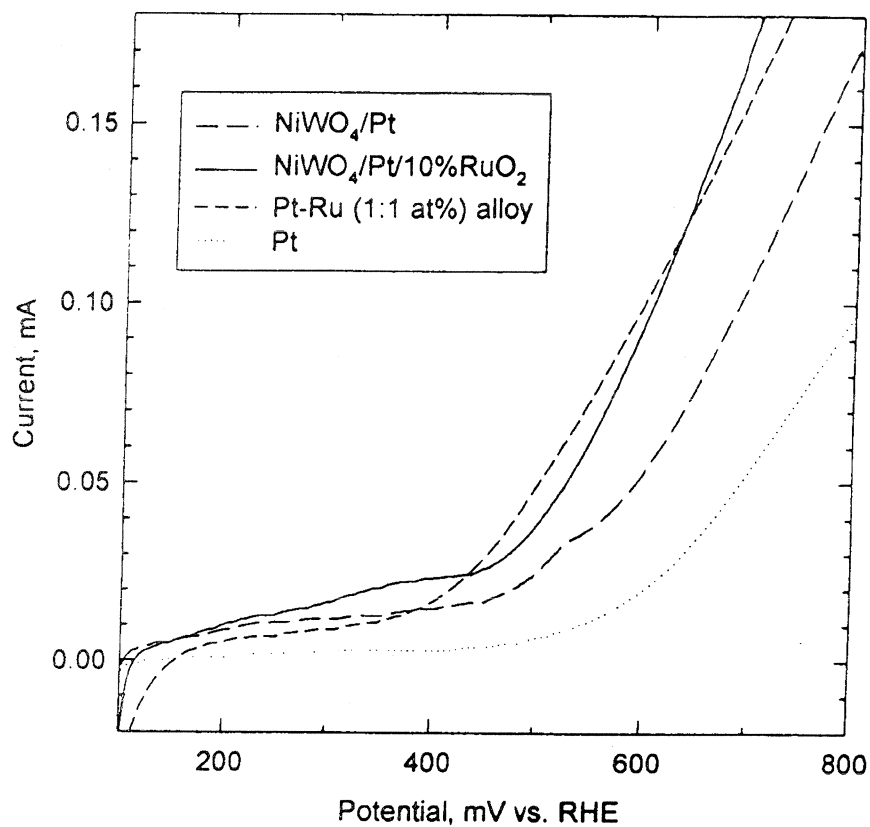
N.S.Marinkovic et al., "In situ Infrared Spectroscopic Investigations...", Figure 3.

N.S.Marinkovic et al., "In situ Infrared Spectroscopic Investigations...", Figure 4.

24

a)

b)

N.S.Marinkovic et al., "In situ Infrared Spectroscopic Investigations...", Figure 5.

-ΔR/R   0.05%

wavenumbers, cm^{-1}

N.S.Marinkovic et al., "In situ Infrared Spectroscopic Investigations…", Figure 6.

N.S.Marinkovic et al., "In situ Infrared Spectroscopic Investigations...", Figure 7.

N.S.Marinkovic et al., "In situ Infrared Spectroscopic Investigations...", Figure 8.

Methanol oxidation curves on different catalysts

Figure axes:
- Y-axis: Current, mA (0.00, 0.05, 0.10, 0.15)
- X-axis: Potential, mV vs. RHE (200, 400, 600, 800)

Legend:
- — — · NiWO$_4$/Pt
- ——— NiWO$_4$/Pt/10%RuO$_2$
- - - - Pt-Ru (1:1 at%) alloy
- ········· Pt

solution: 0.5M H2SO$_4$ + 0.5M CH$_3$OH;

approx. surface area: 1.42 cm^2;
equal ammount of Pt in each catalyst;
all catalysts are supported by
Carbon(Vulcan)/37% PTFE mixture.

VOLUME 98-1

Meeting Abstracts

San Diego

May 3 – 8, 1998

THE 193RD MEETING OF

The Electrochemical Society, Inc.

om
4 Fe³⁺, 0.2 mM Fe²⁺
4ClO₄

400   800
SE / mV

potential curve of the
RDE. Potentials given vs.
ctrode (MSE). Potential of
)₄ on this scale is -0.46 V.

-200   0
mV

the logarithm of the
of the Fe³⁺/Fe²⁺ reaction

In situ spectroelectrochemical investigation of CO adsorption on underpotentially deposited silver at Pt(111) electrode

N.S. Marinkovic, J.X.Wang and R.R. Adzic

Department of Applied Science, Brookhaven National Laboratory, Upton, NY 11973

CO adsorption on a metal poly- and monocrystalline surfaces has been one of the major subjects of surface science for decades (1). Upon adsorption on transition metal electrodes, the CO stretching vibration is shown to be lowered from the gas phase value of 2138 cm^{-1}. This behavior is explained in the Blyholder model by a weak electron transfer from 5σ CO orbital followed by a stronger back-donation from the transition metal d-band into the $2\pi^*$ CO orbital. In the case of 1B transition metals, this back donation is of minor importance because of the low lying d-band. Therefore, CO is known to be physisorbed on bulk silver electrodes, and only an indication of a weak chemisorption is found (2). A chemisorption of CO has been reported on 30-atoms long Ag clusters, and the value of CO stretching frequency is found to be lowered to 2080 cm^{-1} (3). It is expected that even stronger shift to the red would be found on smaller Ag clusters and especially on monolayer and bilayer Ag electrodes.

Mono-and bilayers of silver on platinum electrodes have been obtained in the way described earlier (4). The spectroelectrochemical measurements were conducted in a custom made cell with a ZnSe hemispherical window (5), placed in an external chamber of a Mattson RS-10000 spectrometer. PAR-273 potentiostat was used to set the potential of the working electrode alternatively to the reference or the sample value.

Underpotential deposition of silver on Pt(111) occurs in the potential region 0.65 - 1.2 V vs. RHE (4) in two steps. In solution of 1mM Ag$^+$ + 0.05 M H$_2$SO$_4$, the monolayer is formed in a broad potential region between 1.2 and 0.95 V. The bilayer is formed at 0.69 V, 30 mV before the onset of bulk deposition (4). When this solution is saturated with CO, the cyclic voltammogram in Figure 1 shows that the electrochemical oxidation proceeds at the UPD monolayer of Ag in a wide potential region. In the anodic scan, the CO oxidation commences at 0.9 V and shows a maximum at 1.07 V. In the cathodic direction, the CO oxidation takes place in a potential region that extends up to the onset of bilayer formation.

Fig. 2 shows the *in-situ* adsorption and electrooxidation spectra of CO at the silver monolayer at a Pt(111) electrode. The reference scan was taken at 0.7 V, just before the onset of bilayer formation, and the sample scans were taken at more positive potentials, starting from 0.8 V and incremented by 0.1 V. A bipolar band with a negative lobe at 2020 cm^{-1} and a positive one at ~2050 cm^{-1} arises as a consequence of a C=O stretching frequency change when the potential is switched from the reference to the sample value. The positive lobe appears to shift to higher frequencies as the electrode potential is made more positive. At the potentials higher than 1.0 V, a sharp, positive-going band at 2343 cm^{-1} appears in the spectra due to the CO$_2$ formation at the electrode surface.

These results clearly indicate that the CO is chemisorbed on Ag monolayer in a potential region that extends up to the onset of Ag bilayer formation, and is oxidized at potentials more positive than 0.9 V. Its chemisorption and oxidation can be easily followed by means of *in situ* spectroelectrochemistry.

References:
1. F.M.Hoffmann, Surf.Sci.Reports, 3 (1983) 107.
2. W.Hanson, M.Bertolo and K.Jacobi, Surf.Sci., 253 (1991) 1.
3. F.W.Froben, I.Rabin, M.Ritz and W.Schultze, Z.Phys. D, 335 (1996) 338.
4. N.S.Marinkovic, J.X.Wang and R.R.Adzic, in: "The Electrochemical Double Layer", Proc. Electrochem. Soc., Vol. 97-17, Pennington, NJ (1997).
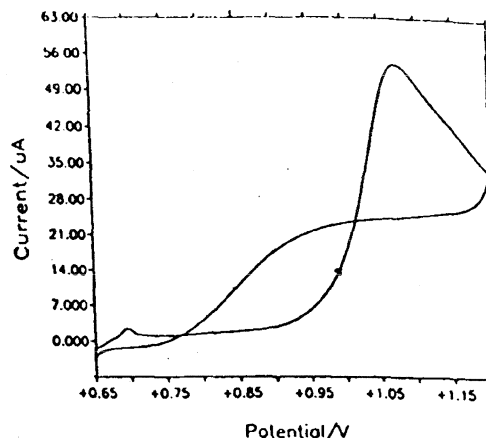5. N.S.Marinkovic, J.S.Loring, M.Hecht and W.R.Fawcett, Electrochim.Acta, 41 (1996) 641.

Figure 1. Cyclic voltammetry of CO oxidation on the monolayer of silver deposited at a Pt(111) in a CO-saturated solution of 1 mM AgSO$_4$ + 0.05 M H$_2$SO$_4$. Sweep rate 2 mV s^{-1}.

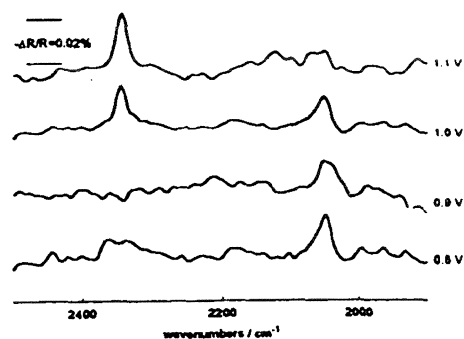**Figure 2.** SNIFTIRS spectra of CO adsorption/oxidation on the UPD Ag /Pt(111) in CO-sauturated solution of 1 mM AgSO$_4$ + 0.05 M H$_2$SO$_4$. Reference scan was taken at potential of 0.7 V, and sample scans were taken at potentials as indicated in the figure. 768 scans, 8 cm^{-1} resolution, p polarization.